Correlation between optical characteristics and NO_2 gas sensing performance of ZnO nanorods under UV assistance

Thi Thu Do[1*], Thi Hien Hoang[2,3], Thi Anh Thu Do[1*], Quang Ngan Pham[1], Hong Thai Giang[1], Ha Trung Bui[2], Trung Tran[2], Truong Giang Ho[1]

[1]Institute of Materials Science, Vietnam Academy of Science and Technology
[2]Hung Yen University of Technology and Education
[3]Graduate University of Science and Technology, Vietnam Academy of Science and Technology

Received 11 July 2017; accepted 10 October 2017

Abstract:

In this research, we present the ZnO nanorods synthesized through the simple route of the hydrothermal method. The ZnO nanorods were developed through the application of only zinc acetate $Zn(CH_3COO)_2$ and ammonia solution, NH_4OH, in the hydrothermal process at 150^0C for 10 hours. The size of the ZnO nanorods was defined as approximately 300 nm in diameter and 1-2 µm in length. The fabrication of sensors was achieved through drop-coating of synthesized ZnO nanorods on Al_2O_3 substrates integrated with Au electrodes. Subsequent to the process of sintering done at 500^oC for different durations, ZnO nanorod-based sensors were investigated when exposed to NO_2 gas (1.5, 2.5, and 5 ppm) at room temperature under continuous UV-LED (385 nm) illumination. The correlation between NO_2 gas sensing performance and the optical property of the ZnO nanorods is discussed in detail. Herein, the defect concentration, particularly `in the surface region of the ZnO nanorods could be modified through sintering, and this indicates its importance in the reduction of response-recovery times and enhancement of high sensitivity to NO_2 gas.

Keywords: *optical property, room temperature NO_2 gas sensors, ZnO nanorods.*

Classification number: *5.1, 5.5*

Introduction

Nitrogen oxides NO_x (NO_2, NO) are considered highly toxic gases, due to the adverse effects they have on human health as well as the environment. Thus, the analysis and control of NO_x gases is extremely crucial. The gas sensors with high response, fast response-recovery times, and high selectivity with regard to NO_x detection have attracted increased attention in recent times [1]. Nano metal oxide based NO_x gas sensors constituent promising candidates for realistic application in this regard due to advantages such as extremely low detecting level (even up to ppb), high resolution, and fast response. For example, the gas sensors that utilized metal oxides, such as WO_3 [2-4], ZnO [5-7], among others, were found to exhibit an extremely high sensing performance to NO_2 gas. However, the metal oxide based gas sensors usually operate at high temperatures, and subsequently, become unstable or less reliable due to the changing particle size and morphology structure [8]. Therefore, the development of metal oxide gas sensors that operate at room temperature has been emphasized.

Zinc oxide semiconductors with large band gaps (E_g = 3.37 eV) have been applied in many fields such as gas sensors [2-7], photovoltaic devices [9], optoelectronic devices [10], solar cells [11], among others. ZnO nanostructures such as nanosheets, nanorods, nanowires, nanotubes, and nanobelts are mostly utilized for gas sensing layers that operate at low temperatures. This is considered by the relation of their high surface to volume ratio, highly active center, along with other factors [12]. The application of ZnO nanostructures with respect to the detection of various gases such as NO_2 [5-7, 12], CO [13], H_2 [14], and ethanol [15, 16] has been widely investigated. Conversely, to effect a reduction of the operating temperature to room temperature, the application of metal oxide gas sensors with the assistance of UV light has been a mostly feasible approach [17, 18]. S.W. Fan, et al. [17] demonstrated that UV light strongly enhanced the H_2 sensing properties of polycrystalline ZnO at room temperature. Similarly, G. Lu, et al. [18] also indicated that gas sensors based on ZnO nanorods modified SnO_2 nanoparticles have high sensitivity

*Corresponding author: Email: dothianhthu@gmail.com

and fast response-recovery times with regard to NO_2 gas at room temperature, illuminated by UV light. It was suggested that ZnO nanorods could generate photo-electrons into their conduction band under the exposure of UV irradiation. The photo-generated electrons could promote the adsorption of oxygen molecules on the surface of ZnO nanorods. Hence, the gas-sensing responses of the ZnO nanorod based sensors can significantly increase through the application of UV illumination at room temperature.

Recently, the significance of surface defects in ZnO nano oxides with regard to their gas sensing characteristics has been considered [1]. Liao, et al. have investigated that oxygen vacancies in ZnO nanorods dominated the electronic properties and adsorption behaviors, because they acted as donors to provide electrons to the ZnO conduction band [19]. Further, it was found that the defects (oxygen vacancies (V_O); oxygen interstitial (O_i); oxygen antisite (O_{Zn}); zinc vacancies (V_{Zn}); zinc interstitial (Zn_i)) influenced the sensing performance of ZnO-based gas sensors [1, 19, 20]. In general, ZnO nano-oxides' defects can be modified through annealing processes. However, the gas sensing mechanism of the ZnO nano-oxides at room temperature under UV irradiation has not been clearly verified with regard to the contribution of surface defects or bulk defects. Thus, in this paper, the correlation of optical characterizations with gas sensing properties was discussed in detail to provide further evidence related to the gas sensing performance of ZnO nanorods with the assistance of UV light.

Experimental

The ZnO nanorods were synthesized by a simple method. Specifically, zinc acetate $Zn(CH_3COO)_2.2H_2O$ salt (Sigmal-Aldrich 1724703 USP) was dissolved in deionized water through stirring at 80°C for 15 minutes to obtain a homogeneous solution. Subsequently, the NH_4OH solution was gradually dropped into the solution until pH = 9 was attained and continuously stirred for 30 minutes to obtain a mixture that contained white precipitation. Thereafter, the mixture was transferred into a Teflon lined autoclave to grow ZnO nanorods at 150°C for 10 hours by hydrothermal condition. Finally, the precipitation mixture was filtered and washed with deionized water until the pH value of 7 was reached, and subsequently dried at 60°C for 24 hours to obtain the ZnO nanorods.

Crystalline structures and surface morphology of ZnO nanorods were characterized by X-ray diffraction (X'Pert Pro) using CuKα radiation, scanning electron microscope (FESEM, HITACHI S-4800). The optical characterization of ZnO nanorods was identified by photoluminescence (PL) emission spectra when excited by 325 nm light from a Cenon lamp at room temperature.

The ZnO nanorods were mixed with an organic (α-terpineol: antarox: ethyl-cellulose = 95:2:3) to obtain a paste. The ZnO nanorods paste was drop-coated on the Al_2O_3 substrates integrated with Au grid-electrodes. Fig. 1 illustrated the process from synthesizing the ZnO nanorods, fabricating sensor devices and illuminating UV-LED light to gas sensors. To measure gas sensing performance, these sensors were sintered at 500°C for different durations to obtain the devices for subsequent analyses. UV-LED light source (wavelength = 385 nm) was adjusted for the irradiation intensity via the applied currents (1, 5, and 15 mA) to investigate gas sensing performance of the sensors. The sensors were continuously irradiated with the UV light during the measurement of the gas sensing characteristics. The sensors were measured with the current source (Keithley, model 6220) and the voltage meter (Keithley, model 2700) for data acquisition of the sensor resistance when exposed upon NO_2 gas concentrations under UV irradiation. The response (S) of the ZnO nanorod sensors was calculated by the equation $S=(R_g-R_a)/R_a \times 100$, where R_g and R_a are the sensor resistances in the air containing NO_2 gas and in air respectively.

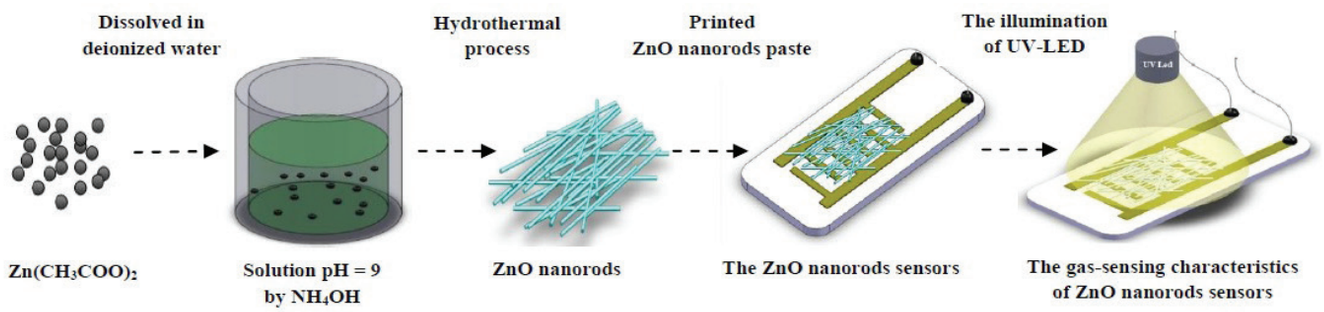

Fig. 1. Diagram illustrated procedure of synthesizing the ZnO nanorods, fabricating the sensor devices, and illuminating UV-LED to the ZnO nanorods sensors.

Results and discussion

Figure 2 displays the SEM image of the typical morphology of the synthesized ZnO nanorods sample. It can be observed that the sample contains uniform nanorods with 300 nm diameter and 1-2 µm length. It is found that the ZnO nanorods are hexagonal rod-shaped, as described in the inset in Fig. 2.

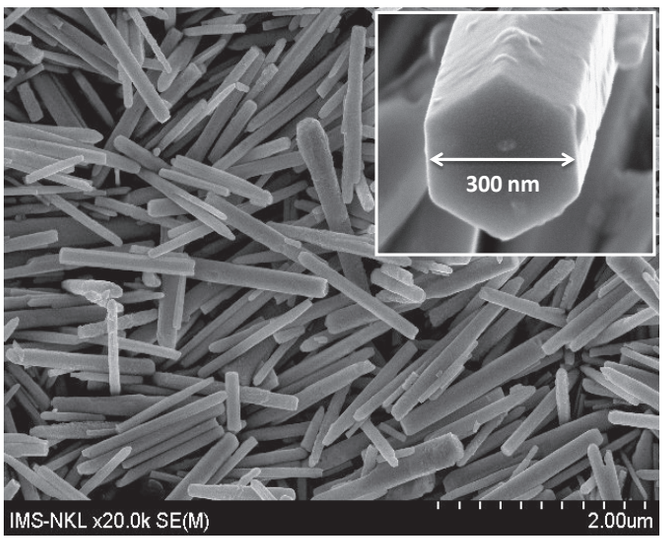

Fig. 2. SEM image of the ZnO nanorods synthesized through the hydrothermal process.

Figure 3 displays XRD patterns of the ZnO nanorod as-grown and after sintering at 500^{0}C for 24 hours. All the diffraction peaks can be indexed to typical hexagonal Wurtzite structure, in accordance with the JCPDS card (No. 36-1451). No diffraction peaks for any impurity phases are found in the XRD patterns. In addition, the position and proportion of the diffraction peaks are found to be very similar when the as-grown and sintered samples are compared. This result suggests that crystalline structure and crystalline particle-size of the ZnO nanorods can be preserved even after the long sintering process conducted at 500^{0}C.

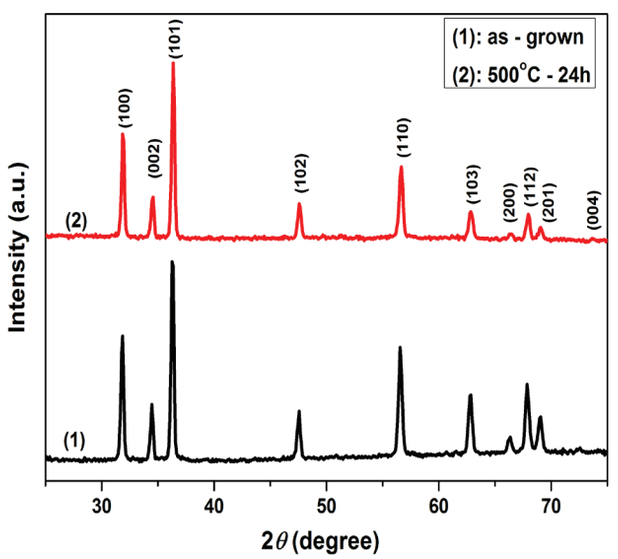

Fig. 3. XRD patterns of the ZnO nanorods as-grown and sintered at 500^{o}C for 24 hours.

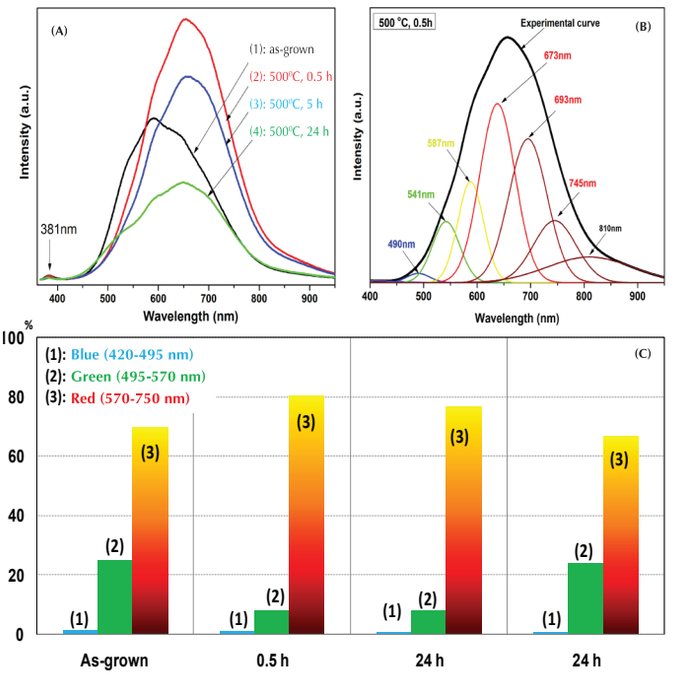

Fig. 4. PL spectra of the ZnO nanorods as-grown and sintered at 500^{o}C for 0.5, 5, and 24 hours (A); the typical Gaussian deconvolution of the ZnO nanorods sintered at 500^{o}C for 0.5 hours (B); the calculated percentage chart of blue (420-495 nm), green (495-570 nm), and yellow-red (570-750 nm) emissions of the samples (C).

It has been generally suggested that the five defects observed in the ZnO oxides include oxygen vacancies (V_O), oxygen interstitial (O_i), oxygen antisite (O_{Zn}), zinc vacancies (V_{Zn}), and zinc interstitial (Zn_i), in which V_O and Zn_i are donors and O_i, O_{Zn} and V_{Zn} are acceptors. These defects can be proofed through the photoluminescence properties. Fig. 4A shows the PL spectra of the ZnO nanorods sintered at 500^{o}C for 30 minutes, 5 hours, and 24 hours. Evidently, all the samples have the two emission bands with a weak band of 381 nm (assigned to near band gap emission of the ZnO nanorods) and broad visible band of 400-750 nm. The visible emission band is assigned to the deep defects in ZnO nanorods [1, 19-21]. Fig. 4B displays the typical Gaussian deconvolutions of the PL spectra in the range of 400-950 nm of the ZnO nanorods sintered conditions at 500^{o}C for 0.5 hours. The blue, green, yellow-red emissions are calculated in accordance with the assigned defects that occur in bulk and surface of the ZnO oxide. From the Gaussian deconvolution of the PL spectra, the calculated percentage of the emissions area is summarized for each wavelength ranges as described in Fig. 4C. The blue and green emissions band are considered in relation to oxygen antisite (O_{Zn}) or zinc vacancies (V_{Zn}) that is corresponded to the deep defects levels in the ZnO band-gap [22, 23]. Whereas, the yellow-red emissions are assigned for oxygen vacancies (V_O) that operate as donors, the behavior that has also been regarded with respect to the effect of the V_O^{++} surface defects [24-26].

These defects can be considered as important contributions to the electrical conductivity and gas sensing characteristics of the ZnO nanorods. The percentage of the yellow-red emissions are found to have maximum value for ZnO nanorods sintered at 500°C for 0.5 hours, and it gradually reduces with increasing sintering time (as seen in Fig. 4C). The result in Fig. 4C shows that the concentration of oxygen interstitial (O_i), oxygen antisite (O_{Zn}), zinc vacancies (V_{Zn}), which can be assigned as the bulk defects [26], decreased after sintering for short durations (0.5 and 5 hours), and then increased with the increase in sintering up to 24 hours.

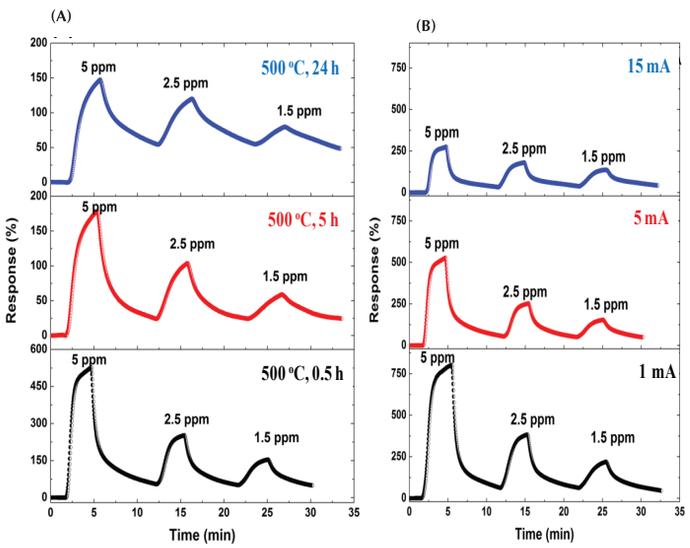

Fig. 5. Responses to NO_2 gas at room temperature of the ZnO nanorods based sensors with sintering for 0.5, 5, and 24 hours (A); with applied currents of 1, 5, and 15 mA to the UV-LED (B).

Figure 5A displays the NO_2 gas-sensing responses of the ZnO nanorod sensors sintered at 500°C for 0.5, 5, and 24 hours under UV-LED (385 nm) illumination with 5 mA applied current at room temperature. The results indicate that the responses of all the ZnO nanorod sensors increase when exposed upon NO_2 gas. This behavior is related to ZnO nanorods as *n*-type semiconductor. From the result, it is observed that the sensors with long sintering duration show the small responses to NO_2 gas.

Figure 5B presents the response to NO_2 gas at room temperature of ZnO nanorods sensor sintered 500°C for 0.5 hours when current values of 1, 5, and 15 mA are applied to the UV-LED. The result demonstrates that the response of this ZnO nanorods sensor reduces with increase in the currents applied to the UV-LED. To further analyze gas sensing performance, Fig. 6A presents the dependence of the response of the ZnO nanorods sensor on sintering time under measuring conditions of exposure to 5 ppm NO_2 gas and the application of 5 mA to the UV-LED. It was discovered that the NO_2 response has maximum value for the ZnO nanorods based sensor for 0.5 hours sintering time, and it strongly decreases with the above given sintering time. The dependence of the response-recovery times of the ZnO nanorods sensor on sintering time under measuring conditions of exposure to 5 ppm NO_2 and application of 5 mA to the UV-LED can be observed in Fig. 6B. The response-recovery times of the ZnO nanorods based sensor increases with increase in the sintering time.

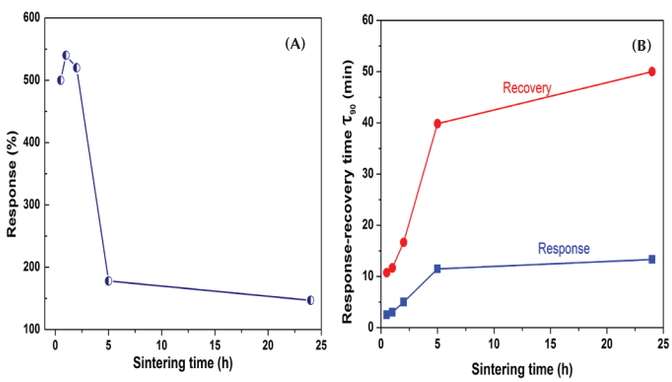

Fig. 6. Dependences of the response (A) and the response-recovery times (B) of the ZnO nanorods based sensors on sintering time under the measuring conditions of exposure to 5 ppm NO_2 and application of 5 mA to the UV-LED.

For gas-sensing mechanism, when the ZnO nanorods are illuminated by the UV-LED, electrons in the valance band or defect levels can move into the conduct band and simultaneously create holes in the valence band. The photo-induced electrons have highly chemical active. Therefore, when the ZnO nanorods exposed to NO_2 gas under UV irradiation, the chemical reactions between NO_2 gas and electrons can occur as following Eqs. (1-3):

$$NO_2(g) + e^-_{hv} \rightarrow NO_2^-(ads) \quad (1)$$

$$NO_2^- + O^-(ads) \rightarrow NO_3^-(ads) \quad (2)$$

$$NO_2 + e^-_{hv} \rightarrow NO + O^-(ads) \quad (3)$$

From these reactions, it can be concluded that the resistance of ZnO nanorod sensors increases when exposed to NO_2 gas, as observed in Fig. 5, due to the electrons extracted from the conduction band. The gas sensing performance of the sensors can be governed by the photo-induced electrons that can move into the oxide surface and participate in the chemical reactions. This can be strongly affected by the surface-structure and surface defects of the ZnO nanorods. Thus, in this research, we have investigated the photoluminescence spectra of the ZnO nanorods sintered at 500°C for difference durations to examine the correlation between the optical properties and the gas-sensing characteristics. As the above results indicate, the sensor with the ZnO nanorods sintered for 0.5 hours exhibited high sensitivity and fast response-recovery times in comparison to others sintered for longer durations. The high concentration of the oxygen vacancies (as donors) can improve the interaction

with the oxidation/reduction gases (NO_2 and O_2 gases).

Conclusions

In conclusion, the ZnO nanorods were synthesized successfully by the simple hydrothermal method at 150°C for 10 hours. The nanorods were 300 nm in diameter and 1-2 µm in length. The ZnO nanorod-based sensors were fabricated to detect NO_2 gas at room temperature under UV-LED irradiation (385 nm) exposure. It was noticeable that when the sensor was sintered at 500°C for 0.5 hours, it exhibited high sensitivity and fast recovery-response times with regard to low NO_2 gas concentration. The correlation between the optical characterizations and the gas sensing properties depended on the concentration of oxygen vacancies in the ZnO nanorods. This sensor can be a promising device that offers room temperature operation for the detection of NO_2 gas in the air.

ACKNOWLEDGEMENTS

This work was funded by the project for youth researcher from Vietnam Academy of Science and Technology (code: VAST.DLT02/15-16) and National Foundation for Science and Technology Development (NAFOSTED, code 104.04-2014.19). The authors wish to express gratitude for the analyses provided at National Key Laboratory for Electronic Materials and Devices, Institute of Materials Science, Vietnam Academy of Science and Technology.

REFERENCES

[1] C. Zou, F. Liang, S. Xue (2015), "Synthesis and oxygen vacancy related NO_2 gas sensing properties of ZnO:Co nanorods arrays gown by a hydrothermal method", *Applied Surface Science,* **353**, 1061.

[2] Z. Hua, et al. (2010), "NO_2 sensing properties of WO_3 varistor-type gas sensor", *Sensors and Actuators B: Chemical,* **150**, 588.

[3] Y. Qin, M. Hu, J. Zhang (2010), "Microstructure characterization and NO_2-sensing properties of tungsten oxide nanostructures", *Sensors and Actuators B: Chemical,* **150**, 339.

[4] M.L. Grilli, et al. (2005), "Planar electrochemical sensors based on YSZ with WO_3 electrode prepared by different chemical routes", *Sensors and Actuators B: Chemical,* **111-112**, 91.

[5] C. Li, et al. (2008), "Fabrication and gas sensing property of honeycomb-like ZnO", *Chinese Chemical Letters,* **19**, 599.

[6] Z. Yang, et al. (2008), "High-performance ethanol sensing based on an aligned assembly of ZnO nanorods", *Sensors and Actuators B: Chemical,* **135**, 57.

[7] E. Oh, et al. (2009), "High-performance NO_2 gas sensor based on ZnO nanorod grown by ultrasonic irradiatio", *Sensors and Actuators B: Chemical,* **141**, 239.

[8] G. Korotcenkov (2008), "The role of morphology and crystallographic structure of metal oxides in response of conductometric-type gas sensors", *Materials Science and Engineering: R: Reports,* **611**.

[9] X.M. Zhang, et al. (2009), "Fabrication of a High-Brightness Blue-Light-Emitting Diode Using a ZnO-Nanowire Array Grown on p-GaN Thin Film", *Advanced Materials,* **21**, 2767.

[10] R. Chakraborty, et al. (2009), "Fabrication of ZnO nanorods for optoelectronic device applications", *Indian Journal of Physics,* **83**, 553.

[11] W.J.E. Beek, M.M. Wienk, R.A.J. Janssen (2006), "Hybrid Solar Cells from Regioregular Polythiophene and ZnO Nanoparticles", *Advanced Functional Materials,* **16**, 1112.

[12] C.J. Chang, et al. (2014), "Ce-doped ZnO nanorods based low operation temperature NO_2 gas sensors", *Ceramics International,* **40**, 10867.

[13] T. Sin Tee, et al. (2016), "Microwave-assisted hydrolysis preparation of highly crystalline ZnO nanorod array for room temperature photoluminescence-based CO gas sensor", *Sensors and Actuators B: Chemical,* **227**, 304.

[14] S. Öztürk, et al. (2014), "Hydrogen sensing properties of ZnO nanorods: Effects of annealing, temperature and electrode structure", *International Journal of Hydrogen Energy,* **39**, 5194.

[15] Y.J. Chen, C.L. Zhu, G. Xiao (2008), "Ethanol sensing characteristics of ambient temperature sonochemically synthesized ZnO nanotubes", *Sensors and Actuators B: Chemical,* **129**, 639.

[16] N.S. Ramgir, et al. (2013), "Ethanol sensing properties of pure and Au modified ZnO nanowires", *Sensors and Actuators B: Chemical,* **187**, 313.

[17] S.W. Fan, A.K. Srivastava, V.P. Dravid (2009), "UV-activated room-temperature gas sensing mechanism of polycrystalline ZnO", *Applied Physics Letters,* **95**, 142106.

[18] G. Lu, et al. (2012), "UV-enhanced room temperature NO_2 sensor using ZnO nanorods modified with SnO_2 nanoparticles", *Sensors and Actuators B: Chemical,* **162**, 82.

[19] L. Liao, et al. (2007). "Size Dependence of Gas Sensitivity of ZnO Nanorods", *The Journal of Physical Chemistry C,* **111**, 1900.

[20] W. Kim, M. Choi, K. Yong (2015), "Generation of oxygen vacancies in ZnO nanorods/films and their effects on gas sensing properties", *Sensors and Actuators B: Chemical,* **209**, 989.

[21] T. Bora, et al. (2016), "Defect engineered visible light active ZnO nanorods for photocatalytic treatment of water", *Catalysis Today,* http://dx.doi.org/10.1016/j.cattod.2016.09.014.

[22] C.H. Tsai, et al. (2008) "Surface modification of ZnO film by hydrogen peroxide solution", *Journal of Applied Physics,* **104**, 053521.

[23] X.L. Wu, et al. (2001), "Photoluminescence and cathodoluminescence studies of stoichiometric and oxygen-deficient ZnO films", *Applied Physics Letters,* **78**, 2285.

[24] J.Q. Hu, Y. Bando (2003), "Growth and optical properties of single-crystal tubular ZnO whiskers", *Applied Physics Letters,* **82**, 1401.

[25] Z. Fan, et al. (2004), "Photoluminescence and polarized photodetection of single ZnO nanowire", *Applied Physics Letters,* **85**, http://dx.doi.org/10.1063/1.1841453.

[26] Sesha Vempati, Joy Mitra and Paul Dawson (2012), "One_step synthesis of ZnO nanosheets: a blue-white fluorophore", *Nanoscale Research Letters,* **7**, doi:10.1186/1556-276X-7-470.